

Conf-9209158--7

Preprint Volume AMS 10th Symposium on  
Turbulence and Diffusion, 29 Sep - 2 Oct, 92

## DIAGNOSTIC DETERMINATION OF BOUNDARY-LAYER CUMULUS CLOUDS USING HAPEX AIRCRAFT DATA

CONF-9209158--7

DE93 002164

Qing Zhang

Boundary Layer Research Team, Dept. of Atmospheric & Oceanic Sci.  
University of Wisconsin, Madison, WI 53706 USA

### 1. INTRODUCTION

Boundary-layer cumulus clouds play an important role in surface energy budget via the interaction between clouds and radiation. In turn the formation and evolution of these clouds are dependent upon the boundary layer turbulence structure.

In this study, HAPEX aircraft sounding and near-surface horizontal flight-leg data are used to calculate the distributions of the mixed-layer height ( $Z_j$ ), the lifting condensation level (LCL), the level of free convection (LFC), and the limit of convection level (LOC). The joint distributions of LCL and  $Z_j$ , and LCL and near-surface virtual potential temperature  $\theta_v$  are used to diagnose boundary-layer cumulus-cloud coverage, which then are compared with HAPEX airborne cloud observations.

The distribution of the convective available potential energy (CAPE) of each air parcel at their LCL and LFC and the CAPE profile of sounding are plotted together, which provide an alternative estimate of cumulus cloud coverage.

### 2. HAPEX FIELD EXPERIMENT

The HAPEX (Hydrologic Atmospheric Pilot Experiment) project was conducted near Toulouse, France in 1986. The NCAR King Air aircraft participated in a special observing period of this experiment between 9 May and 15 July. Twenty-six flights were flown following a fixed pattern within a 100 km X 100 km area during this period (Hildebrand, 1988). Flight 6 on 21 May was selected as the case study for this paper for its suitable cloud conditions and high data quality. It includes five sounding legs and nine near-surface horizontal legs (Fig. 1).

HAPEX-FLIGHT 6 (21 May, 1986)

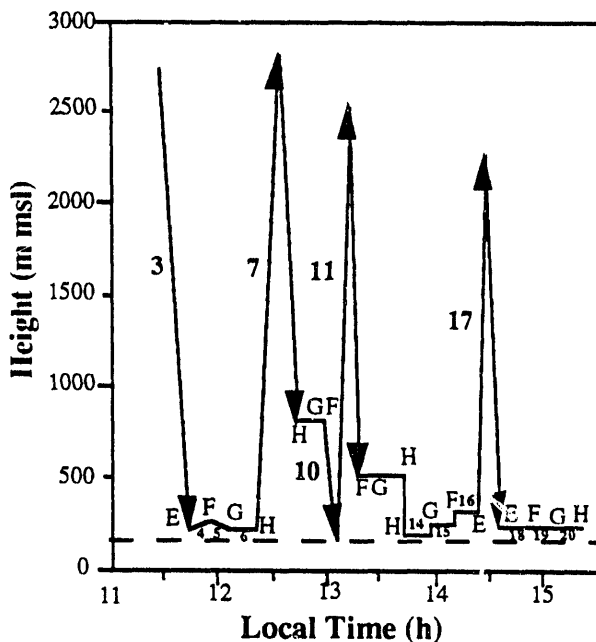


Fig. 1. Flight 6 of the NCAR King Air aircraft during HAPEX on 21 MAY, 1986. The letters E, F, G, and H represent four different locations with different underlying surfaces near Toulouse, which form aircraft flow pattern. The numbers indicate each flight leg. The dashed line shows maximum ground altitude, which is 150 m above mean sea level.

### 3. LCL, LFC, AND LOC DISTRIBUTIONS

MASTER

The soundings of temperature (T), virtual potential temperature ( $\theta_v$ ), and specific humidity (q) were smoothed with a Gaussian filter. The LCL for each data point in the horizontal leg are calculated based on its

DISTRIBUTION OF THIS DOCUMENT IS UNLIMITED

FG0292ER61361

Sc

near-surface measured pressure (P), T, and q. Those data points that are warmer than the environment are considered as rising air parcels. They are lifted dry adiabatically to their LCL and then moist adiabatically to the height of the highest sounding level. The LFC, LOC, and  $Z_i$  of each air parcel are determined by comparing a parcel's  $\theta_v$  with that of the environmental sounding (Stull, 1988).

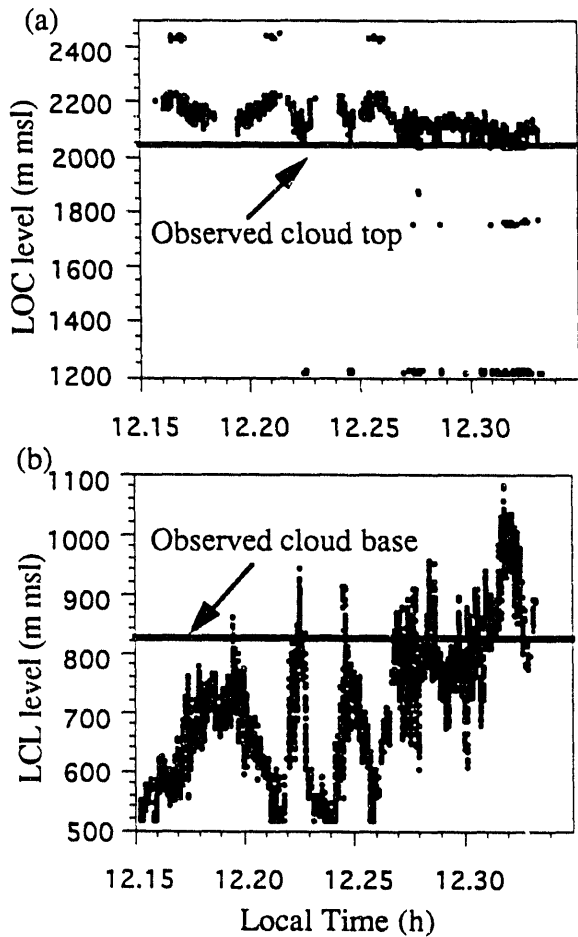


Fig. 2. Distribution of calculated (a) cloud top (LOC) and (b) cloud base (LCL) from horizontal flight leg 6 and sounding leg 7 of Flight 6 in HAPEX. The thick horizontal lines indicate the approximate heights as reported by observers in the aircraft. Each data point represents a 20Hz sample, and there are 12600 samples plotted in this figure.

Distributions of the calculated cloud base height (LCL) and cloud top height (LOC) from near-surface horizontal leg 6 and sounding leg 7 are shown in Fig. 2. The observed average cloud base and cloud top during that period are also plotted as thick horizontal lines. The general agreement between calculation and observation is good; however, the average calculated cloud base is slightly lower than the observation and the

cloud top is higher than the observation. This difference may be caused by neglecting lateral mixing during adiabatic lifting.

Clouds form when parcels' LCLs are lower than their  $Z_i$ . The buoyancy driven boundary-layer cumulus cloud (Cu) coverage can be estimated by using the joint distribution of the parcel's local  $Z_i$  and LCL level (Fig. 3). Among rising parcels, those above the thick line (i.e.,  $LCL < Z_i$ ) contribute to cumulus clouds. The calculated cumulus cloud cover is 37.3%, while the subjective report by observers in the aircraft is 40 - 50% (Stull 1986). Active cumulus cloud cover can be estimated by the number of cloudy points that reach their LFC level. The estimated active cloud cover is 33.6%, while the airborne observation of active Cu is 30 - 50%.

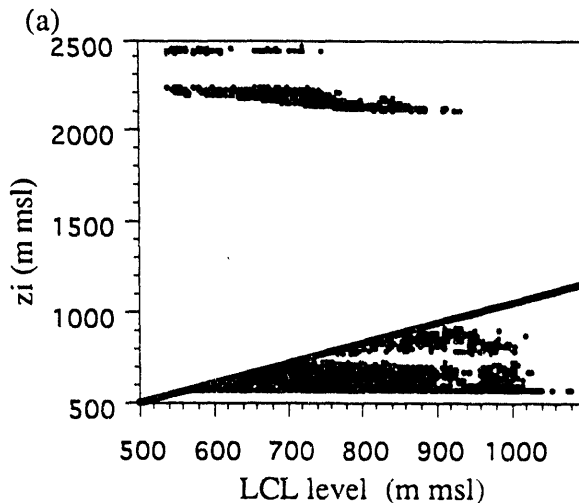


Fig. 3. Joint distribution of  $Z_i$  and LCL for horizontal leg 6 and sounding 7 of Flight 6 in HAPEX. The thick line indicates  $Z_i = LCL$ .

#### 4. $\theta_v$ APPROACH

The  $Z_i$  vs. LCL data such as in Fig. 3 are difficult to use, as noted by Wetzel (1990). An alternative approach is developed in this section that uses easy-to-measure (and hopefully easy-to-parameterize) near-surface data, such as P, T, and q.

Both LCL and  $\theta_v$  (calculated from near-surface measured P, T, and q) of an air parcel are dependent on the properties of the underlying surface, the vegetation, the shape of terrain, and local weather conditions. The joint distribution of LCL and  $\theta_v$  from horizontal leg 6 (above a flat forested area) together with the  $\theta_v$  profile of sounding 7 are plotted in Fig. 4. Fig. 5 displays a similar plot except for horizontal leg 4 (over a hilly farmland) and sounding 3. Those points to the right of the sounding are warmer than the environment and their LCL levels are lower than  $Z_i$ . They can form clouds. Notice that the shapes of the joint distributions for both horizontal legs (Fig. 4 & Fig. 5) have some similarities

and differences that might be possible to parameterize based on surface, weather, and mean boundary-layer conditions. Fig. 6 shows the contours of the joint distribution of LCL and  $\theta_v$  in Fig. 4. The Cu cloud coverage forced by buoyancy can then be diagnosed by overlaying the observed  $\theta_v$  soundings onto the parameterized joint distribution of LCL and  $\theta_v$  for the corresponding surface and weather conditions.

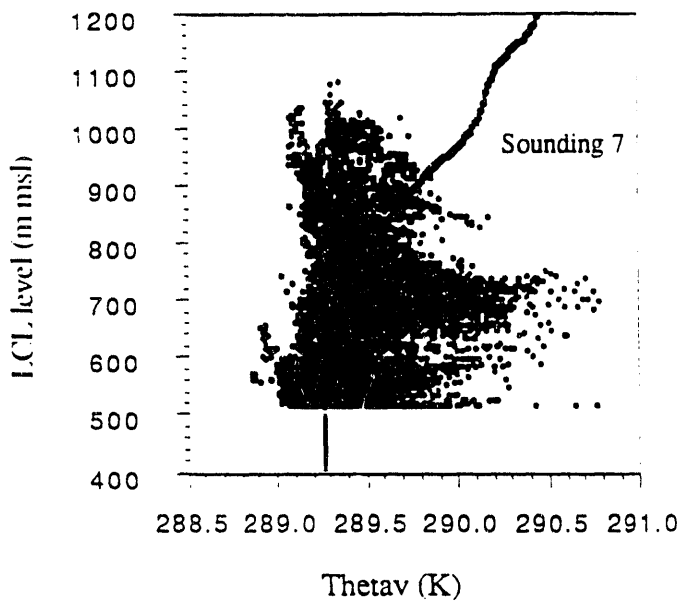


Fig. 4. Joint distribution of LCL and  $\theta_v$  from the near surface horizontal leg 6 and  $\theta_v$  profile of sounding 7.

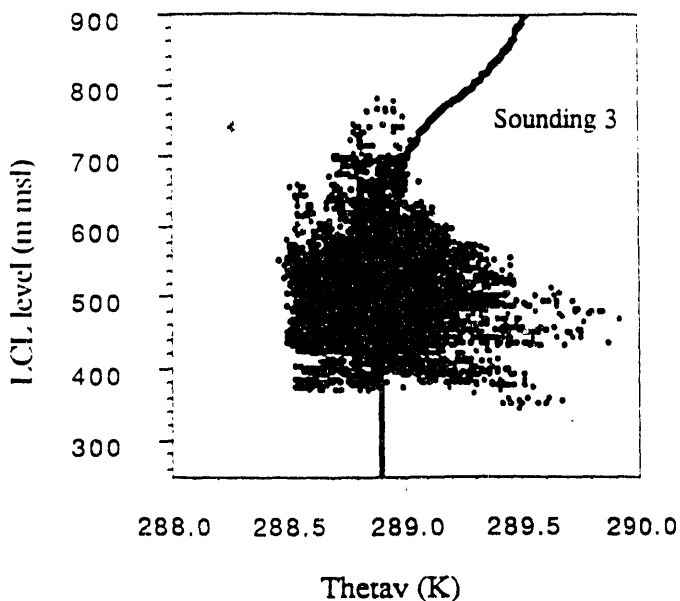


Fig. 5. Same as Fig. 4 except for horizontal leg 4 and sounding 3.

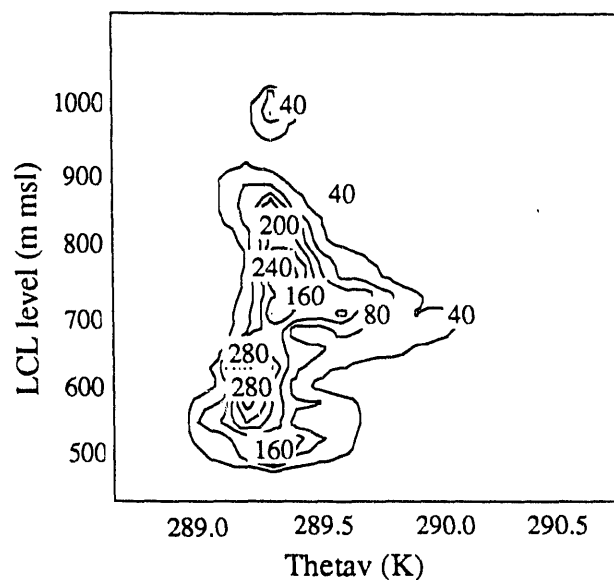


Fig. 6. Contours of the joint distribution of LCL and  $\theta_v$  in Fig. 4.

Techniques such as shown in Figs 4 & 5 consider only the buoyancy of the parcel relative to the environment, but neglect other factors that can contribute to cloud formation such as parcel inertia, background turbulence, and terrain-induced motions. The next section provides an alternative technique into which these other energy sources can be more easily incorporated.

## 5. CAPE APPROACH

Vertical profiles of the convective available potential energy (CAPE) are computed for aircraft soundings and for individual parcels along horizontal legs based on a reference virtual potential temperature ( $\theta_{vr}$ ) (Randall & Wang, 1992) as follows:

$$\text{CAPE}_p|_z = \int_{z=Z_0}^{z=z} \frac{g}{\theta_{vr}} (\theta_{vp} - \theta_{vr}) dz \quad (1)$$

$$\text{CAPE}_s|_z = \int_{z=Z_0}^{z=z} \frac{g}{\theta_{vr}} (\theta_{vs} - \theta_{vr}) dz \quad (2)$$

where  $\text{CAPE}_p$  and  $\text{CAPE}_s$  are CAPE for air parcels and sounding at height  $Z$ .  $Z_0$  is the starting height of sounding and CAPE at  $Z_0$  is assumed to be zero.  $\theta_{vr}$  is chosen as the average measured  $\theta_v$  from the near-surface horizontal leg.  $\theta_{vp}$  and  $\theta_{vs}$  are the potential temperature for air parcels and sounding at height  $Z$ . The difference in CAPE between air parcel and the environment at certain levels indicates the potential convective energy the parcel has at that height. CAPE at LCL and LFC of each parcel for leg 6 and CAPE profile of sounding 7 are plotted in Fig. 7. Similar to Fig. 4, those points to the right of the CAPE profile

are rising at their LCL level (Fig. 7a); therefore, they form cumulus clouds. Those points to the right of CAPE profile in in Fig. 7b form active cumulus clouds. The CAPE method allows other energy sources, such as mechanical turbulence and terrain forcing, to add to the cloud coverage over that from buoyancy alone. The total cloud coverage based on the CAPE method for leg 6 is 65.2% and active cloud coverage is 57.1%. They are closer to the airborne observations than results obtained from the  $\theta_v$  method (see section 3). The  $\theta_v$  method tends to underestimate the cloud coverage because it does not

includes the cloud buoyant inertia, while CAPE tends to overestimate the cloud coverage because it does not consider the friction drag between clouds and their environment. The initial cloud fields are not included in the above calculations.

## 6. CONCLUSION

HAPEX aircraft near-surface horizontal leg and sounding data are used to calculate the lifting condensation level (LCL), the mixed-layer height ( $Z_i$ ), the level of free convection (LFC), the level of limit convection (LOC) for each data point along a horizontal flight leg. The convective available potential energy (CAPE) for horizontal flight leg and sounding are also computed. Two methods are used to determine the buoyancy driven boundary-layer cumulus cloud coverage and type. One approach compares computed LCL's from near surface measurements with the observed local inversion height. Rising parcels with LCLs below the inversion form clouds. The alternative approach examines a parcel's CAPE at their LCL with the environment's CAPE profile. Clouds are formed from parcels with positive buoyancy at their LCL. The  $\theta_v$  approach tends to underestimate cloud formation by neglecting buoyant inertia. The CAPE approach agrees better with the observations in this study and allows for a more complete representation of energy sources of boundary-layer cumulus clouds. These case studies show the start of a larger project with the goal of parameterizing cumulus cloud coverage for use in weather and climate forecast models.

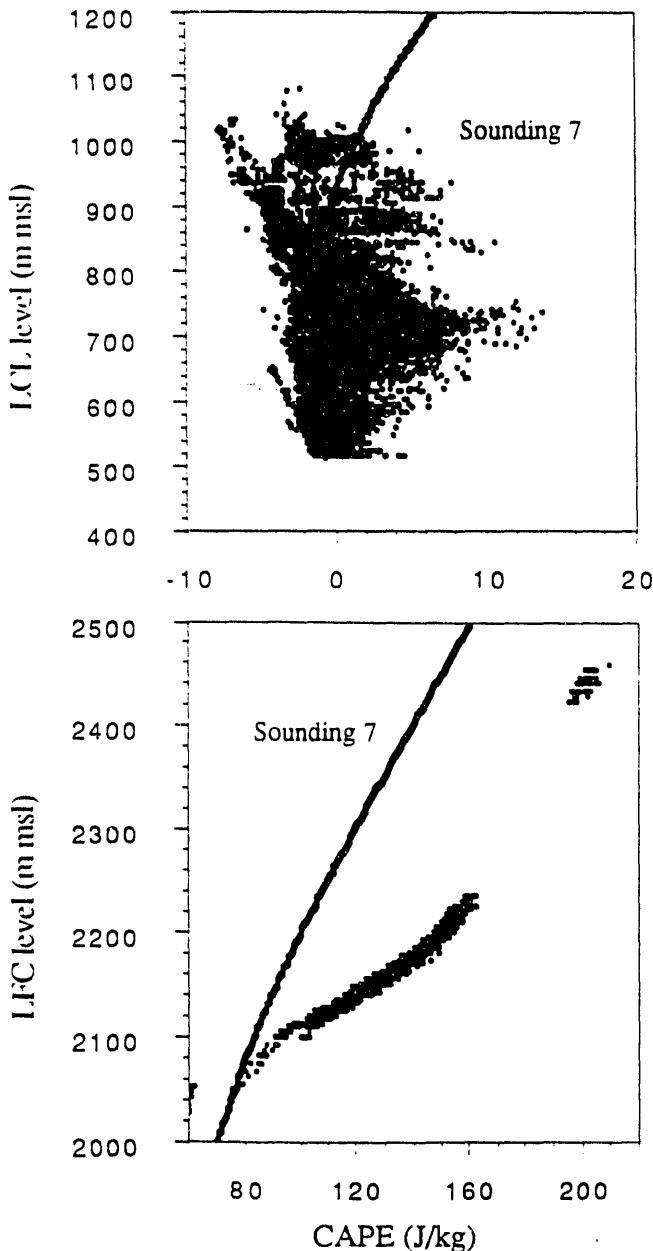


Fig. 7. Joint distributions of (a) LCL with CAPE at LCL and (b) LFC with CAPE at LFC for horizontal leg 6 and the CAPE profile of sounding 7.

**Acknowledgements.** This research was supported by the U.S. Department of Energy under grant DE-FG02-92ER61 361.

## References

- Hildebrand P.H., 1988: *Flux and Sounding Data from the NCAR King Air Aircraft during HAPEX*. NCAR/TN-319+STR, 435 pp.
- Randall, D. A, J. Wang, 1992: *The Moist Available Energy of a Conditional Unstable Atmosphere*, *J. Atmos. Sci.*, **49**, 240-255.
- Stull, R.B., 1986: *Airborne Scientist Flight Logs NCAR King Air N312D*, 63 pp.
- Stull, R.B., 1988: *An Introduction to Boundary-Layer Meteorology*. Kluwer Academic Publishers, Boston, 666 pp.
- Wetzel, P. J., 1990: *Notes and Correspondence A Simple Parcel Method for Prediction of Cumulus Onset and Area-averaged Cloud Amount over Heterogeneous Land Surface*, *J. Appl. Meteor.* **29**, 516-523.

END

DATE  
FILMED  
3/8/93

